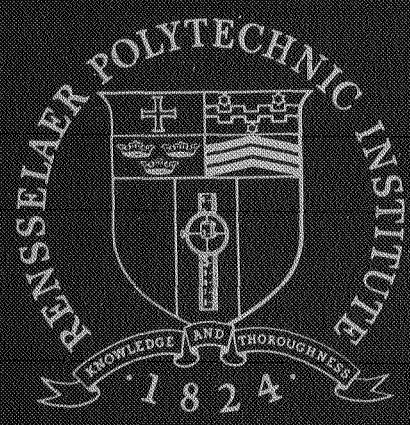


N 69 39 29 7  
NASA CR 106231

CHROMATOGRAPHIC SYSTEMS ANALYSIS:  
SAMPLE INJECTION PROBLEM

Robert C. Krum

CASE FILE  
COPY



Rensselaer Polytechnic Institute  
Troy, New York



## TABLE OF CONTENTS

	Page
	iv
LIST OF FIGURES AND TABLES	
ACKNOWLEDGEMENT	v
ABSTRACT	vi
I. INTRODUCTION . . . . .	1
II. SUMMARY . . . . .	2
III. BACKGROUND . . . . .	5
IV. THEORY . . . . .	9
V. RESULTS AND DISCUSSION . . . . .	14
VI. CONCLUSIONS AND RECOMMENDATIONS . . . . .	37
VII. NOMENCLATURE . . . . .	39
VIII. CITED LITERATURE . . . . .	41
IX. APPENDIX: COMPUTER PROGRAMS . . . . .	42



LIST OF FIGURES .

		Page
Figure 1	Idealized Model . . . . .	18
Figure 2	Comparison of the first order model and pentane chromatogram. . . . .	21
Figure 3	Effect of $mR_0$ on resolution - first order model . . . . .	23
Figure 4	Effect of $N_{tog}$ on resolution - first order model . . . . .	25
Figure 5	Comparison of the equilibrium adsorption model and pentane chromatogram. . . . .	28
Figure 6	Equilibrium adsorption model with high diffusion . . . . .	30
Figure 7	Effect of $P_e$ on resolution - equilibrium adsorption model ( $mR_0 = 0.5$ ). . . . .	32
Figure 8	Effect of $P_e$ on resolution - equilibrium adsorption model ( $mR_0 = 0.2$ ). . . . .	33
Figure 9	Effect of $P_e$ on resolution - equilibrium adsorption model ( $mR_0 = 0.038$ ). . . . .	34
Figure 10	Effect of $mR_0$ on $\theta_\gamma$ - equilibrium adsorption model . . . . .	35

LIST OF TABLES

		Page
Table I	$mR_0$ as a function of various compounds. . . . .	16
Table II	Summary of column parameters used in testing first order model . . . . .	20

## ACKNOWLEDGEMENT

The author wishes to express sincere appreciation to his project advisor, Professor Peter K. Lashmet, whose assistance and guidance was an important part in the preparation of this project. Acknowledgement is also given to Mr. Eric Suggs of JPL and Dr. Stephen Yerazunis, overall NASA Mars project director at RPI for their suggestions and comments, and to the DuPont Corporation for financial assistance in the form of an Industrial Traineeship.

## ABSTRACT

Many of the chemical/biochemical/biological experiments proposed for the unmanned Mars Voyager missions require a general-duty, chromatographic separator for fractionating complex chemical mixtures prior to chemical analysis by a mass spectrometer or other device. Because of the complexity of such a separator, a system analysis based on the mathematical simulation of the chromatograph is being undertaken. Models for an isothermal, packed chromatograph column for use with a single component system have been derived but failed to completely describe the entire output chromatogram. The effect of forcing functions other than the impulse function, used to derive the various models, on chromatogram resolution was investigated in this report. The analysis showed that sample injection has a sizeable, but varying, effect on the output chromatograms. The sharper the peak resolution obtained with the theoretical impulse input, the quicker that resolution was lost as a function of sample injection time. Correlations relating the injection time to loss in resolution for various column parameters in the second order, equilibrium model have been prepared. Once the final advanced mathematical model having the required accuracy needed for system studies has been developed, similar correlations can be prepared using the techniques described in this work.

## INTRODUCTION

One important phase of the initial Voyager missions to Mars is the search for organic matter and living organisms on the martian surface. The present concept for attaining this objective consists of subjecting samples of the atmosphere and surface matter to certain chemical and biologically-related reactions and thereafter analyzing the products produced. The most likely system for a general chemical analysis appears to be a combination gas chromatograph/mass spectrometer. This unit would be a major component in the biological and chemical laboratory of an unmanned, remotely controlled roving lander for Mars. It is the objective of the Chromatographic Systems Analysis program to generate fundamental engineering design techniques and system concepts for use in optimizing the design of such a chromatograph separation system. Such a system should provide maximum resolution with minimum retention times and minimum carrier gas usage and should be capable of separating components evolving from many different kinds of experiments.

Because of the variety of the mixtures to be separated and the complexity of the fractionating process, a system analysis based on the mathematical simulation of the chromatograph is being undertaken. The technique will use mathematical models, which will incorporate fundamental parameters evaluated from reported experiments, to explore various concepts and to direct further experimental research.

## PART II

## SUMMARY

A mathematical model describing a single component isothermal chromatograph was developed from the basic differential equations which govern rates of mass transport in packed columns. Neglecting second order diffusional effects, a solution was obtained which adequately predicted retention times but failed significantly in predicting peak spreading. Since a reasonably accurate model is required for systems evaluation, new studies were undertaken to investigate two probable causes of peak spreading: gaseous diffusion effects neglected in the first order model, and injection of the sample in finite periods of time. The latter topic is the subject of this report.

The forcing function chosen for study was that of a step pulse which was convoluted with the solution of the first order model developed for an impulse forcing function. Due to the complexity of the integral resulting from the convolution, a computer program was developed to evaluate the integral as a function of time by numerical methods. This technique was also applied to a special solution of the diffusional second order model in which the number of transfer units was set equal to infinity (equilibrium adsorption).

The results of the above analysis showed that sample injection has a sizeable, but varying, effect on the



output chromatogram. Basically, increasing injection time has two effects. First, since the injection function was more diffuse than the theoretical impulse function, the output functions were broader, and shorter, than those associated with the impulse function. The loss in resolution varied with column parameters; however, as a general rule the sharper the theoretical impulse peak, the quicker that resolution was lost as a function of sample injection time. The second effect of injection time was the movement of the theoretical peak appearance time to later values as the injection time increased.

Information concerning the effect of diffusion on the mathematical model was also obtained when the equilibrium adsorption model of the second order system was studied. Even though diffusional effects in the system under study were known to be small, inclusion of these effects greatly influenced the shape of the resulting chromatograms. A complete solution of the second order model should further improve the predicting of output chromatograms, hopefully to the position where the required accuracy needed for system studies can be obtained.

The technique of convoluting a pulse injection function with a mathematical model obtained using an impulse injection has proved feasible. Further studies using other mathematical representations of the injected function can

be accomplished; however, it will be more important to study the effect of injection upon the advanced mathematical model now being developed. Correlations concerning the loss in resolution as a function of sample injection time and column parameters must be developed using the advanced model if detailed system studies are to have value.

PART III  
BACKGROUND

The initial work in the field of chromatographic system analysis was done by Sliva (4) who derived a mathematical model for an isothermal, packed chromatograph column for use with a single component system. Basically, the system works as follows. A tube is packed with a granular solid, having dimensions greatly smaller than the tube diameter, upon which a high molecular weight, non-volatile liquid, which acts as an adsorbent, is coated. Continuously flowing through the column is a carrier gas which is not adsorbed by the liquid coating. The materials to be separated are injected into the carrier gas stream and are adsorbed by the liquid as the injected pulse flows down the column. The adsorbed materials will then desorb when the pure carrier gas, upstream of the injected pulse, passes over them. Separation of the various materials results since different materials adsorb and desorb at different rates depending upon the thermodynamics of the system. Therefore, when a composition detector is mounted at the end of the column, a peak for each component will appear.

The derivation of the dimensionless differential equation governing the operation of a gas chromatograph was accomplished by performing a material balance on a differential element of the column using the following

assumptions:

1. The column is isothermal.
2. The carrier gas velocity profile is flat.
3. The axial diffusion coefficient,  $D$ , is a composite factor which may or may not have a turbulent component.
4. The gas composition is approximately constant in the direction normal to flow, and the concentration gradient occurs only in a thin boundary layer near the adsorbent; i.e., mass transfer coefficients could be used.
5. The adsorbent layer is so thin that there is no diffusional resistance within the layer in the direction normal to the surface.
6. The diffusivity in the adsorbent layer is so small that there is no diffusion in the direction parallel to the surface (in the axial direction).
7. The net rate of adsorption for the carrier gas is negligible.
8. Only one component is adsorbed and its gaseous phase composition is very small.
9. The carrier gas behaves as an ideal gas.

Three equations are required to express the behavior of the adsorbing component: a mass balance for the gas phase, a mass balance for the adsorbent (liquid) phase, and a thermodynamic function relating the gas-phase and adsorbed-phase concentrations. The respective equations in terms of dimensionless variables are\*:

$$\frac{1}{Pe} \frac{\partial^2 y}{\partial z^2} - \frac{\partial y}{\partial z} - N_{tog} (y - y^*) = \frac{\partial y}{\partial \theta} \quad (\text{III-1})$$

$$\frac{1}{R_0} \frac{\partial X_L}{\partial \theta} = N_{tog} (y - y^*) \quad (\text{III-2})$$

$$y^* = mX_L \quad (\text{III-3})$$

Gaseous diffusion of the adsorbing compound in

---

\*See Part VII for nomenclature.



the direction of carrier gas flow is represented by the second derivative appearing in Eq. (III-1). For an initial solution of the above three equations, the gaseous diffusion effects were considered to be second order effects. Therefore, the coefficient of the second derivative in Eq. (III-1) was set equal to zero. The solution in the Laplace transform domain to the above set of equations for the case of no axial diffusion is as follows:

$$y(z,s) = A(s) \exp \left[ -N_{\text{tog}} z - sz + \frac{N_{\text{tog}} z}{(s/mR_o N_{\text{tog}} + 1)} \right] \quad (\text{III-4})$$

For an impulse sample injection, Eq. (III-4) inverts to the following:

$$\begin{aligned} y(z,\theta) &= 0 & \theta < z \\ &= \frac{N(v/L)}{W} \exp \left[ -N_{\text{tog}} z \right] \exp \left[ -(\theta-z)mR_o N_{\text{tog}} \right] \cdot \\ &\quad \left[ 2 N_{\text{tog}}^2 z mR_o \frac{I_1(x)}{x} + \delta(\theta-z) \right] & \theta > z \end{aligned} \quad (\text{III-5})$$

The argument  $x$  is defined as:

$$x = 2 \sqrt{N_{\text{tog}}^2 z (\theta-z) mR_o}$$

The above equation has been designated as the first order mathematical model of the gas chromatograph.

Eq. (III-5) was compared to actual chromatographic data (4), and was able to predict the retention time of the sample but it failed significantly in predicting peak spreading. Since a reasonably accurate model is required for systems evaluation, new studies were undertaken to

investigate two probable causes of peak spreading: gaseous diffusion effects neglected in the first order model, and injection of the sample in finite periods of time. The latter topic is the subject of this report.

At the time this report was completed, a complete solution of Eqs.(III-1), (III-2), and (III-3) including the gaseous diffusion term had not been accomplished. However, a special case in which  $N_{\text{tog}}$  was infinite had been solved and is known as the equilibrium adsorption model (6). The solution is:

$$\begin{aligned}
 y(z, \theta) &= 0 && \theta < z \\
 &= \frac{N(v/L)}{W} \frac{1}{2} \sqrt{\frac{B \text{Pe}}{\pi \theta^3}} \exp\left[\frac{\text{Pe}}{2}\right] \exp\left[-\frac{\text{Pe} \theta}{4 B}\right] \exp\left[-\frac{\text{Pe} B}{4 \theta}\right] && \theta > z
 \end{aligned} \quad (\text{III-6})$$

$$\text{where } B = 1 + \frac{1}{mR_0}$$

This equation was also derived considering the sample to be injected in the form of an impulse.

This study is concerned with the effects of finite sample injection time upon the mathematical models represented by Eq.(III-5) and Eq.(III-6).

PART IV  
THEORY

In order to determine the effect of forcing functions other than an impulse upon output resolution, we decided to use the first order model, Eq. (III-5), as our first point of analysis. The choice of this model was made for two reasons. First, the first order model is the least complicated mathematical expression we have which attempts to describe an output chromatogram. By use of this model, we hoped to obtain qualitative correlations between column parameters ( $N_{tog}$ ,  $mR_0$ ) and sample injection time. Secondly, at the time this project was started, a complete solution to the second order model was not available. Once the techniques of analyzing the effect of sample injection on output resolution are developed for the simpler first order model, they can then be applied to more complicated mathematical expressions such as the equilibrium adsorption second order model, Eq. (III-6)..

The forcing function chosen for study is that of a step pulse. The reason for this choice is that the step pulse will most probably be a good representation of the forcing function associated with a mechanical injection unit, which will be necessary on a roving lander.

The Laplace transform form of a step pulse input is (4):

$$A(z,s) = \frac{N(v/L)}{\theta_r W} \frac{1}{s} (1 - \exp[-\theta_r s]) \quad (\text{IV-1})$$

$\theta_r$ , the dimensionless injection time, is defined as:

$$\theta_r = \frac{\tau v}{L}$$

much the same way as the dimensionless time  $\theta$  is defined.  $\tau$  represents the time for sample injection.

It should be noted that the limit of Eq. (IV-1) as  $\theta_r$  approaches zero is that of an impulse function where the sample size, as a dimensionless quantity, is defined by  $N(v/L)/W$ .

The problem is now to determine how this pulse function affects the first order model described by Eq. (III-5). Multiplication of the transform of the first order model Eq. (III-4) by the transform of the pulse input Eq. (IV-1) gives:

$$g(z,s) = y(z,s) A(z,s)$$

or

$$g(z,s) = \frac{N(v/L)}{\theta_r W} \left[ \frac{y(z,s)}{s} - \frac{y(z,s)\exp(-\theta_r s)}{s} \right] \quad (\text{IV-2})$$

It will be noticed that the above equation for  $g(z,s)$  consists of the difference between two terms. The terms are exactly the same except that the second term is delayed by an amount equal to the sample injection time. Therefore, the ability to invert  $y(z,s)/s$  as a function of



$\Theta$  will permit solution of Eq. (IV-2) in the time domain.

The solution of  $y(z,s)/s$  will be done by the method of convolution (1):

$$\mathcal{L}^{-1} \left[ \frac{y(z,s)}{s} \right] = \int_0^{\Theta} y(z,\gamma) F(z,\Theta-\gamma) d\gamma$$

where  $F(z,\Theta-\gamma) = \mathcal{L}^{-1} \left[ \frac{1}{s} \right] = 1$

Therefore, we have to evaluate the following integral:

$$J = \int_0^{\Theta} y(z,\gamma) d\gamma$$

Substitution of Eq. (III-5) gives as the integral:

$$J = \int_0^{\Theta} \exp \left[ -N_{\text{tog}} z - (\gamma-z)mR_0 N_{\text{tog}} \right] \cdot \left[ 2N_{\text{tog}}^2 z m R_0 \cdot \frac{I_1(x)}{x} + \delta(\gamma-z) \right] d\gamma \quad (\text{IV-3})$$

The integral is composed of two terms, one associated with the Bessel function and one associated with the delta-function. The contribution by the delta-function term may be shown to be:

$$\exp \left[ -N_{\text{tog}} z \right] \exp \left[ N_{\text{tog}} z m R_0 \right]$$

by substituting the definition of the delta-function into the integral and performing the integration. It will be noted that this part of the integral is not time dependent. Referring back to Eq. (IV-2), it will be seen that the above expression will appear in both terms and, since it is not dependent on time, will cancel itself out. Therefore, with

specific reference to solving Eq. (IV-2), the integral can be reduced to:

$$J = \int_0^{\theta} \exp \left[ -N_{\text{tog}} z - (\gamma - z)mR_0 N_{\text{tog}} \right] \left[ 2N_{\text{tog}}^2 z mR_0 \cdot \frac{I_1(x)}{x} \right] dz \quad (\text{IV-4})$$

To make the integral more manageable, the following change of variable was made:

$$\lambda = 2\sqrt{N_{\text{tog}}^2 z(\gamma - z)mR_0}$$

Substitution of the above variable change into Eq. (IV-4) yields:

$$\int_0^{2\sqrt{N_{\text{tog}}^2 z(\theta - z)mR_0}} \exp \left[ - \left( \frac{\lambda}{2\sqrt{N_{\text{tog}} z}} \right)^2 - N_{\text{tog}} z \right] I_1(\lambda) d\lambda \quad (\text{IV-5})$$

Note that when the lower limit was changed, the new lower limit was a negative number. However, negative times have no effect on the integral since the sample is injected at time equal to zero. Hence, the lower limit can be set to zero.

An attempt to solve Eq. (IV-5) analytically by expanding the Bessel function,  $I_1(\lambda)$ , in a series expansion and integrating term by term failed. The resulting series was too bulky and converged too slowly to be useful. Therefore, a computer program was written (see appendix) to numerically evaluate the above integral as a function of  $\theta$ . The output listed the time domain solution of  $y(z,s)/s$  as a function of  $\theta$ . Therefore, a resulting point on the output chromatogram generated by a step pulse forcing

function could be found by the following formula:

$$g(z, \theta) = \frac{N(v/L)}{\theta_r W} \left[ F(\theta) - F(\theta - \theta_r) \right] \quad (\text{IV-6})$$

where  $F(\theta)$  is the computer program output of the solution of Eq. (IV-5) evaluated at  $\theta$ .

A completely analogous derivation can be performed on the equilibrium adsorption model. For this model, described by Eq. (III-6), the integral became:

$$J = \int_0^{\theta} \frac{1}{2} \sqrt{\frac{B Pe}{\pi \lambda^3}} \exp \left[ \frac{Pe}{2} \right] \exp \left[ -\frac{Pe \lambda}{4 B} \right] \exp \left[ -\frac{Pe B}{4 \lambda} \right] d\lambda$$

This integral was also solved by a computer program using the technique developed for the first order model. The output from this program is, as before, a listing of the time domain solution of  $y(z, s)/s$  as a function of  $\theta$ . Hence, Eq. (IV-6) can be used to generate the required output chromatograms.

## PART V

## RESULTS AND DISCUSSION

In studying the first order model, we are primarily interested in determining, in a qualitative manner, the effect sample injection time has on the output chromatogram. We hope to be able to develop techniques of analysis and some basic correlations relating injection time and column parameters to the chromatogram which can then be applied to more complicated models. Before evaluating the results of a step pulse forcing function, it would be useful to review the effect various column parameters have on output resolution for an impulse injection function. A more complete description of these effects appeared in the earlier studies (4).

The two major column parameters which describe output resolution are the number of transfer units  $N_{tog}$ , a dimensionless quantity related to the efficiency of the adsorption process, and  $mR_0$ , a thermodynamic function related to component volatilities. The magnitude of  $N_{tog}$  is affected by carrier gas velocity, particle diameter and column length. Decreasing the first two and increasing the latter will increase the value of  $N_{tog}$ . Large values of  $N_{tog}$  cause the chromatogram peak to become sharp, leading to good resolution. Low values cause short, broad peaks which may tend to overlap, thus decreasing resolution.

The time of peak appearance, with no axial diffusion,



is a direct function of  $mR_0$ . This is shown by taking the equation for the first order model in the transform domain and determining the limiting case by setting  $N_{tog}$  equal to infinity. Thus Eq. (III-4) becomes in the limit as  $N_{tog}$  approaches infinity:

$$y(1,s) = A(s) \exp \left[ -s \left( 1 + \frac{1}{mR_0} \right) \right] \quad (V-1)$$

The above equation shows that for  $N_{tog}$  equal to infinity, the forcing function,  $A(s)$ , will appear exactly as injected at a later time  $( 1 + 1/mR_0 )$ . Hence, the theoretical time of peak appearance,  $\theta_m$ , for the idealized system can be defined as:

$$\theta_m = 1 + \frac{1}{mR_0} \quad (V-2)$$

If axial diffusion is present,  $\theta_m$  will also have a dependence on the Peclet number,  $Pe$ , a measure of the amount of diffusion (2,6).

$mR_0$  can therefore be considered a measure of relative component volatilities since highly volatile substances will appear first. Each component however, does not have a unique  $mR_0$ . Temperature, pressure, and the type of adsorbing substrate used are all factors in the determination of  $mR_0$  for a specific chromatograph. Table I shows approximately how  $mR_0$  varies for different compounds when using a column composed of a liquid substrate of 20% by weight silicone grease on a 60/80 mesh chromosorb packing at one atm. pressure and 50°C.(3). It can readily be seen in the alkane series

TABLE ImR<sub>0</sub> as a Function of Various Compounds

<u>Compound</u>	<u>mR<sub>0</sub></u>
Methane	15.0
Ethane	3.7
Propane	1.5
Butane	0.56
Pentane	0.23
Hexane	0.092
Heptane	0.038
Octane	0.015
Ethylene	7.5
Propylene	1.8
Isobutylene	0.62
1-Butene	0.62
trans-2-Butene	0.52
cis-2-Butene	0.45
1-Pentene	0.26
trans-2-Pentene	0.21
cis-2-Pentene	0.20
1-Hexene	0.10
trans-2-Hexene	0.089
cis-2-Hexene	0.081

Conditions: Silicone grease, 20% by weight on 60/80  
 mesh chromosorb  
 1 atm. pressure  
 50°C.

that as component volatility increases,  $mR_0$  increases causing earlier theoretical peak times.

For a constant  $N_{tog}$ , some output resolution is lost as  $mR_0$  decreases. Theoretical impulse peaks for pentane ( $mR_0 = 0.23$ ) are sharper than peaks for hexane ( $mR_0 = 0.092$ ), when all other variables are kept constant (4).

To begin the analysis of sample injection, consider the case of the ideal column described by Eq. (V-1). In this column there is no diffusion and an infinite number of transfer units. Therefore, the forcing function will appear unchanged at  $\theta_m$ . Figure 1 shows the output of various input functions for a sample size  $A(t)$  of 0.05 and an  $mR_0$  of 0.2 ( $\theta_m = 6$ ). Two items should be noted from this figure. First, the area under each of the peaks is the same in all cases and is equal to the sample size. Secondly, peaks for the step pulses are not centered around the theoretical peak time,  $\theta_m$ , but start at  $\theta_m$ . The reason for this is that the leading edge of the pulse input cannot reach the end of the column any faster than the impulse function. Since the front edge of the pulse input starts at  $\theta = 0$  and ends at  $\theta = \theta_r$ , the front edge must appear at  $\theta = \theta_m$  and end at  $\theta = \theta_m + \theta_r$ . If this analysis is carried over to real systems, we would expect theoretical peak appearance time to move as sample injection time increases.

In order to be able to compare the chromatograms resulting from the first order model with those from an actual system, it was decided to use the same column parameters used in the previous evaluation of the model (4) and summarized in

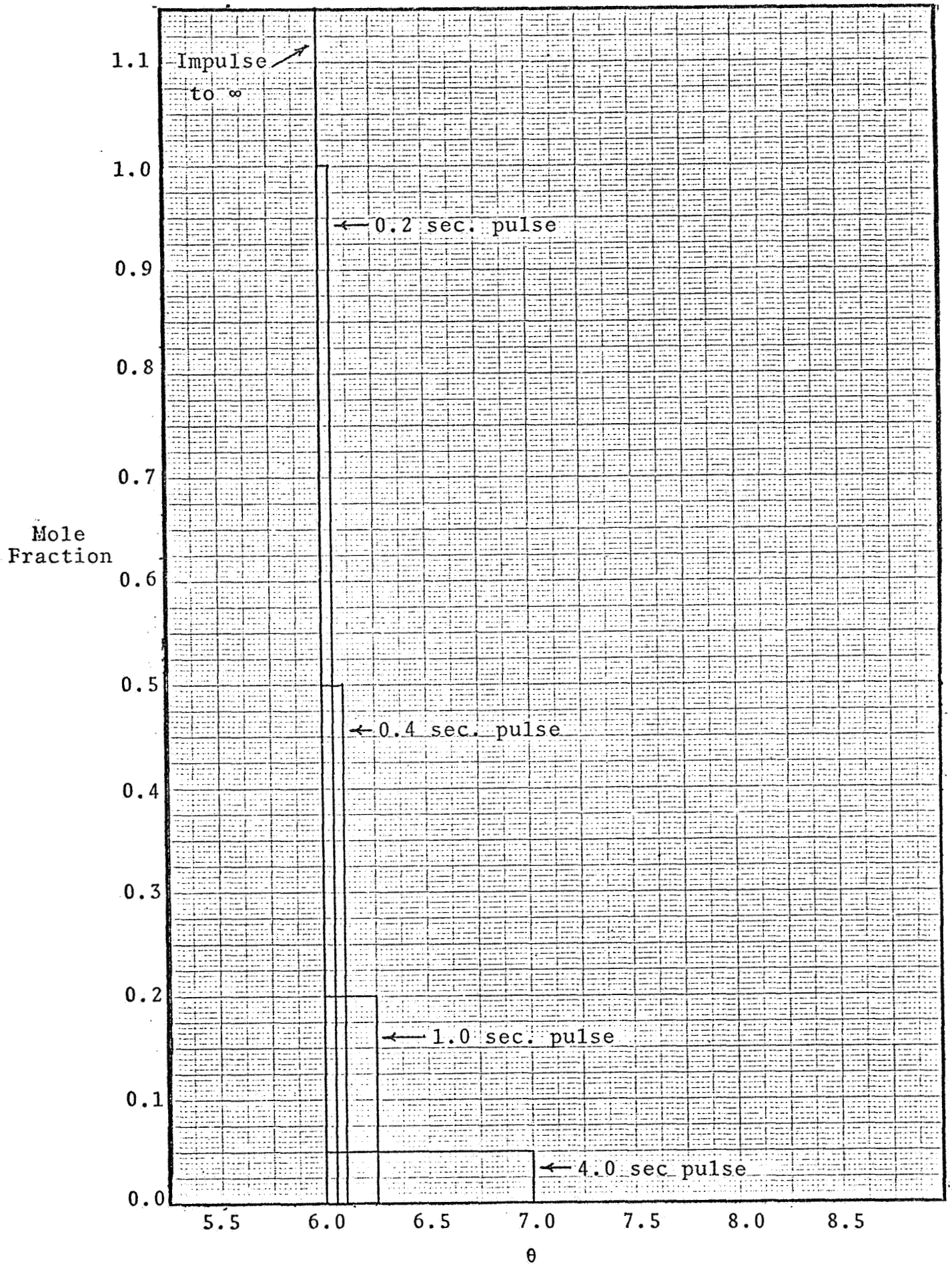


Figure 1: Idealized model -  $mR_0 = 0.2$ ,  $A(t) = 0.05$ ,  $v/L = 0.25$



Table II. The results of a step pulse injection of various times are shown in Figure 2. The curve labeled "actual" was obtained by injecting a liquid pentane sample, by means of a syringe, into the column described in Table II.

As predicted, when sample injection time increases, the time of the maximum point moves to a larger value. The impulse peak is centered around  $\theta = 6$  as described by Eq. (V-2). However, the one second pulse peak is centered around  $\theta = 6.125$  which is the exact time the one second pulse peak of Figure 1 is centered around. As expected, resolution is lost as sample injection time increases. Peak height is lowered with the resulting broadening of the peak base since the area under each curve must remain constant.

Another point of interest is that the basic symmetry of the impulse peak is not lost. The one second pulse peak is just as symmetrical as the impulse peak. Secondly, the peaks all start to appear about the same time. Even though the base of the one second pulse peak is much wider than the impulse peak, the initial parts do not overlap. This further supports the statement that the leading edges of all input functions do reach the end of the column at the same time if axial diffusion is not present.

To show the influence of column parameters upon sample injection effects, it will be necessary to develop a correlation between  $\theta_r$  and the loss in resolution. The amount of resolution, as compared to a peak obtained using a theoretical impulse injection, can be measured by two

TABLE II

Summary of Column Parameters used  
in Testing First Order Model

Length, cm.	61.0
Diameter, cm.	0.46
Particle diameter, cm.	0.0214
Void fraction	0.4
Surface area, cm <sup>2</sup> /cm <sup>3</sup>	168
Temperature, °C	50.0
Pressure, atm.	1.0
Carrier gas flow rate cu. cm./sec.	1.0
Carrier gas velocity cm./sec.	15.23
$\frac{N(v/L)}{W}$	0.05
N <sub>tog</sub>	14,300

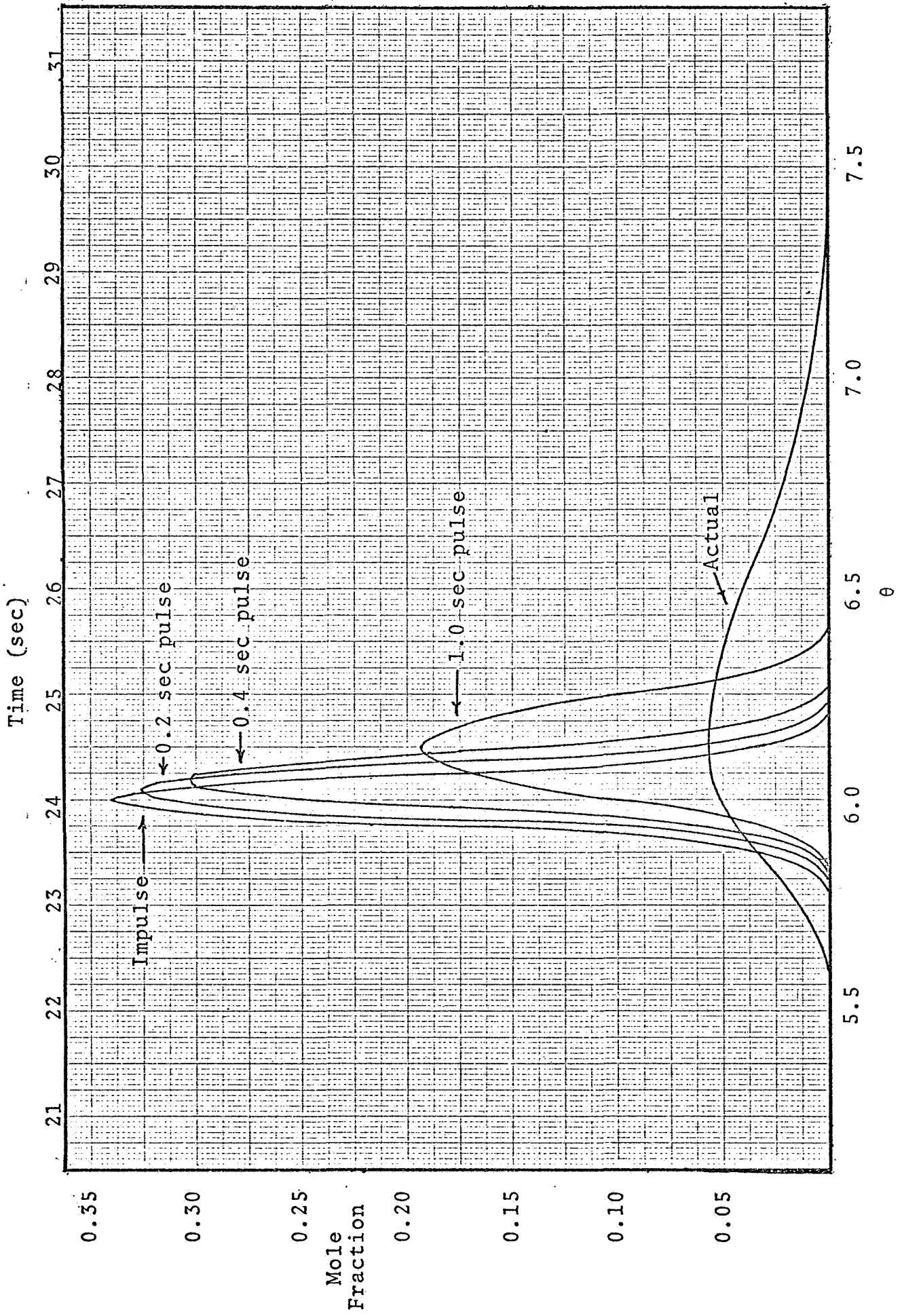


Figure 2: Comparison of the first order model with the pentane chromatogram.

$mR_0 = 0.2$ ,  $N_{\text{tog}} = 14,300$ ,  $A(t) = 0.05$

methods. Either the ratio of peak heights (pulse/impulse) or the amount of base broadening can be used. At first glance, it would be assumed that the amount of base broadening should be used since overlap of the peak bases is the direct cause of resolution problems. However, since the curves are symmetrical and the area under each curve is a constant, the loss in peak height can be directly related to the base broadening. Also, the measurement of peak height can be made very accurately, while the exact starting and ending points on the base of the curve may be difficult to measure, depending upon the amount of accuracy desired. Therefore the decision to use the ratio of peak heights as a measure of the loss in resolution was made. Since the appearance time for the impulse peak is characteristic of the system, a correlation concerning resolution should reflect this fact. Therefore, instead of plotting the ratio of peak heights against  $\theta_r$  alone, a ratio of  $\theta_r/\theta_m = \theta_r / (1 + 1/mR_0)$  is used. Figures 3 and 4 are two plots using the above correlation showing the effect sample injection time has on output resolution as column parameters are varied.

Figure 3 shows the above correlation as  $N_{tog}$  is held constant and  $mR_0$  is varied. It can be seen that the loss of resolution as sample injection time increases is fairly constant as  $mR_0$  is changed. The loss is not as noticeable for low values of  $mR_0$ ; however, the initial resolution of the impulse peak for a low value of  $mR_0$  is not as sharp as that for a higher value of  $mR_0$ . This

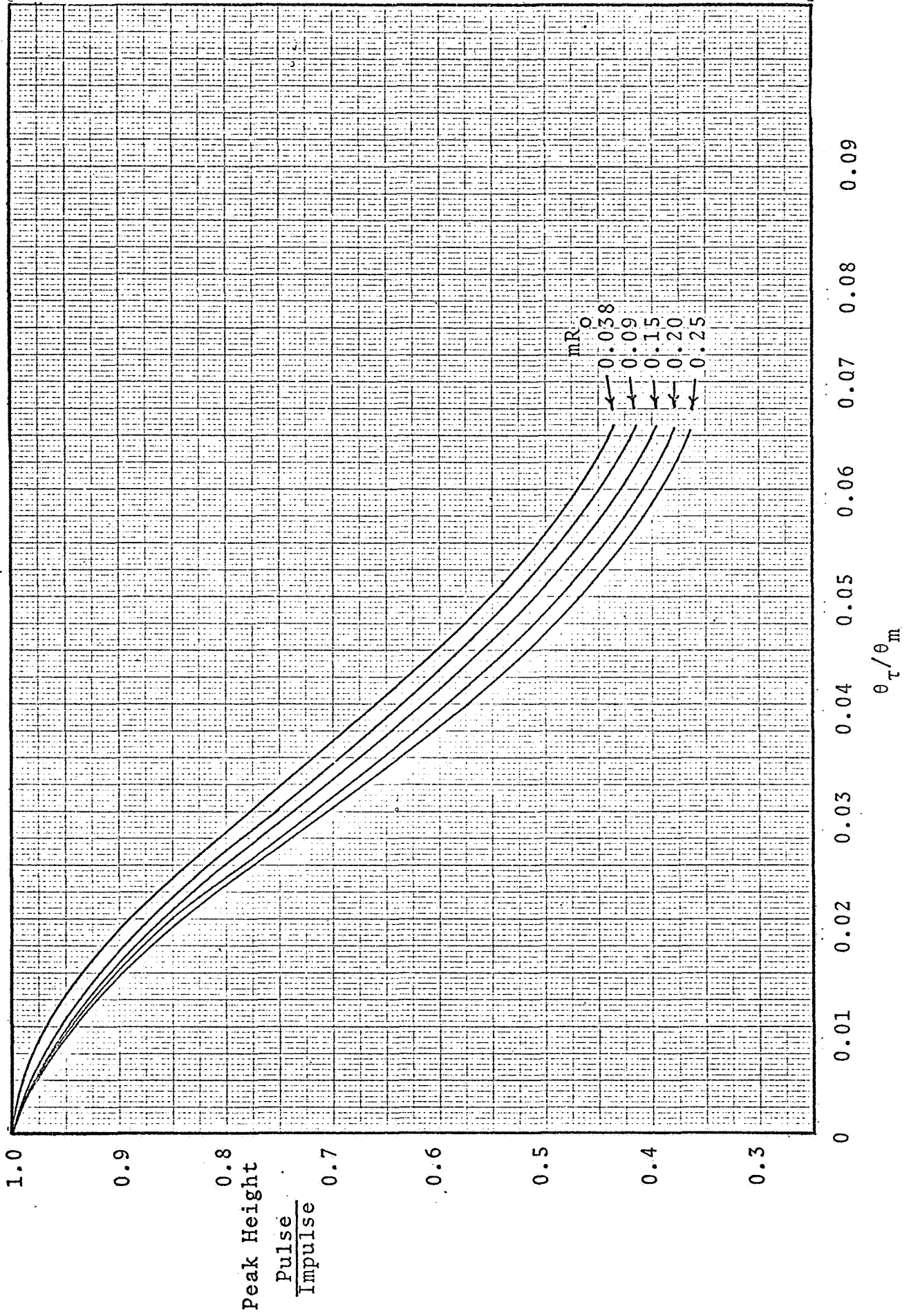


Figure 3: Effect of  $mR_0$  on resolution - first order model,  $N_{\text{tog}} = 14,300$

correlation is useful in the following manner. Suppose a set of operating conditions is specified for the lander chromatograph. Consider also that the thermodynamic properties,  $mR_0$ , of a set of compounds to be detected are known; e.g. two compounds having values of  $mR_0$  of 0.25 and 0.20 respectively. With the quality of the detection system available, suppose a ratio of pulse peak height to impulse peak height of 0.85 might be tolerated in detecting the two compounds. If the peak height ratio is less than 0.85, enough resolution is lost so that detection is uncertain. Referring to Figure 3, it can be seen that for a 0.85 ratio  $\theta_r/\theta_m$  is 0.02. This means that if the theoretical time of peak occurrence of one of the compounds is 20 seconds, then the sample injection time must be less than 0.4 seconds in order to achieve a 0.85 peak height ratio.

Figure 4 shows the effect of  $\theta_r$  on resolution as a function of  $N_{tog}$ . This plot points out one major fact concerning the effect of sample injection time. It will be noticed that for a low value of  $N_{tog}$  sample injection has very little effect on output resolution. However, at low  $N_{tog}$  the impulse peak has extremely poor resolution as shown in the previous studies (4). The impulse peak for an  $N_{tog}$  of 1000 is a very short broad curve which is equivalent to almost no resolution. The impulse peak for an  $N_{tog}$  of 50,000, on the other hand, is extremely tall and narrow. In fact, it is almost a spike peak. This is the type of peak we desire for maximum resolution. However,

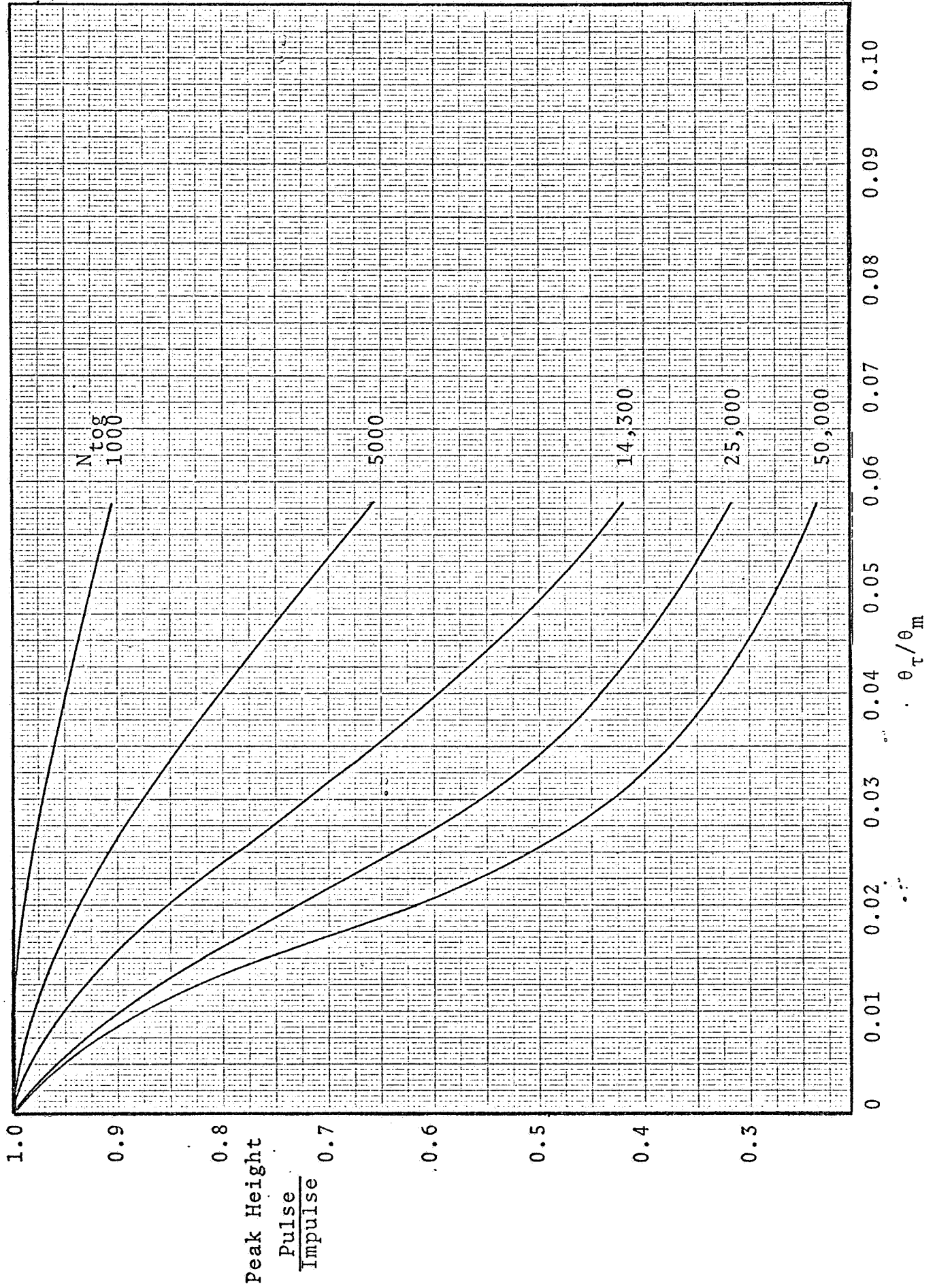


Figure 4: Effect of  $N_{tog}$  on resolution - first order model,  $mR_0 = 0.20$

the resolution for a curve with an  $N_{tog}$  of 50,000 is very quickly lost to sample injection time. In fact, if  $\theta_m$  corresponds to a theoretical peak time of 20 seconds, with an  $N_{tog}$  of 50,000, a step pulse input of only 0.5 second causes the output peak to be one-half the height of the theoretical impulse peak. This emphasizes the general effect, which was also noted in Figure 3: the sharper the theoretical impulse peak, the quicker the resolution is lost as a function of sample injection time.

Since it is known that the first order model fails significantly in predicting the chromatogram even with the addition of sample injection time (Figure 2), it was decided to expand the analysis to a special case of the second order model which had been solved. By doing this we hoped to accomplish three objectives. First, by means of a special second order model, we hoped to generate chromatograms which would more accurately describe the actual system. Secondly, the special second order system would allow correlations on the Peclet number  $Pe$ , a measure of the axial diffusion. Finally, we wanted to show that the technique used to analyze the first order model could be applied to other mathematical models so that when the final model is developed, a procedure for analysing the effects of sample injection would be available.

The special case of the second order model is that of equilibrium adsorption (infinite  $N_{tog}$ ). It is hoped that this assumption of an infinite number of transfer units is



not far from reality since the value of  $N_{tog}$  used in the test system was equal to 14,300. This large value of  $N_{tog}$  in the first order model gave theoretical impulse peaks which were tall and narrow, approaching the spike peak obtained for infinite  $N_{tog}$ .

An estimate of the Peclet number for the test column was obtained ( $Pe = 3000$ ) and used to generate the results shown in Figure 5. This figure is the equilibrium adsorption counterpart of Figure 2. Both figures have the same ordinates for comparison purposes. One item should be kept in mind when comparing Figures 2 and 5. High values of  $Pe$  mean low diffusion, and the upper limiting value of  $Pe$  at high flow rates is about 3000 (2). Therefore, Figure 5 is a graph of an output chromatogram from a column in which diffusional effects are relatively small. The first order model was derived considering the effect of diffusion was negligible. However, Figure 5, when compared to Figure 2, shows that even though diffusional effects may be small, they are extremely influential on the shape of the output chromatogram and must be considered if an accurate mathematical model is to be derived.

The theoretical time of peak occurrence  $\theta_m$  is no longer a simple function of  $mR_0$  as is shown in Eq. (V-2), but is a function of both  $mR_0$  and  $Pe$ . However, the peak occurrence time of the 0.2 second pulse and the one second pulse in Figure 5 is exactly the same as the peak occurrence time of these pulses in Figures 1 and 2. This is further

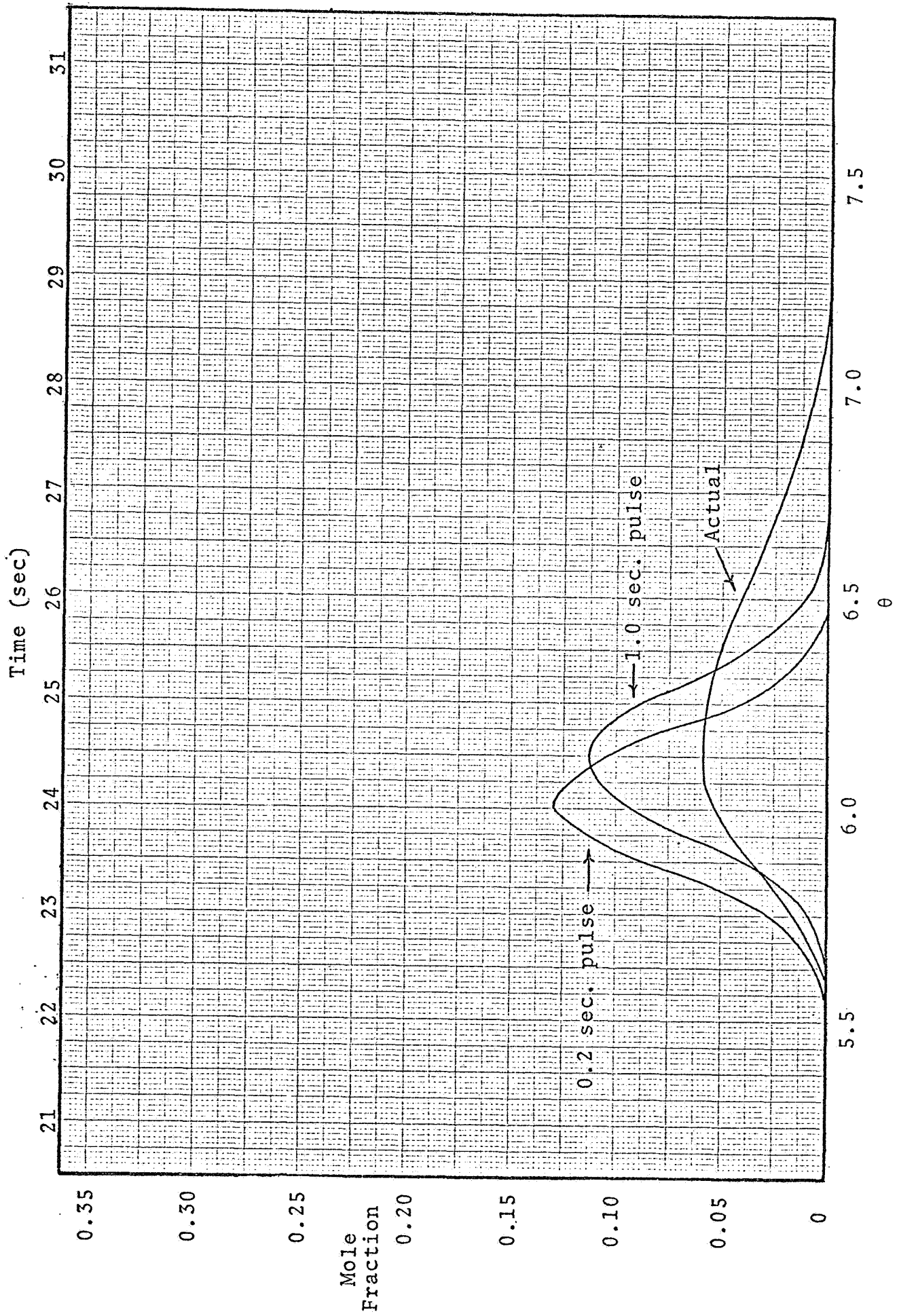


Figure 5: Comparison of the equilibrium adsorption model and pentane chromatogram.

$mR_0 = 0.2$ ,  $Pe = 3000$ ,  $A(t) = 0.05$

proof that diffusional effects are small for this particular case. It should also be noted that the starting point of these peaks is the same as that of the actual chromatogram and the peaks are no longer symmetrical, although they are not as skewed as the actual curve. In summary, the equilibrium adsorption case of the second order model more accurately predicts an actual chromatographic system than does a simple first order model. The addition of  $N_{\text{tog}}$ , i.e. a complete second order model solution, should lower peak heights even further and hopefully be an acceptably accurate mathematical model for use in system studies.

The effect of changing  $Pe$  is shown in Figure 6. The value of  $Pe$  in this figure is 60, meaning a large amount of diffusion is present. Note that the scales of Figure 6 are entirely different from those of Figure 5. If Figure 6 was to be graphed on Figure 5, it would appear almost like a straight line running along the bottom of the plot. This figure is included for three reasons. First, it shows the skewness associated with the diffusional second order model. Secondly, the theoretical peak time is quite different than the corresponding peak times in Figures 1, 2 and 5 showing a dependence of  $\theta_m$  on  $Pe$ . Most importantly, however, is the fact that the only effect sample injection time has on a peak which initially is extremely broad is to move the theoretical peak time to a slightly later value. Both curves in Figure 6 are almost exactly the same except for the time displacement. This plot further supports the

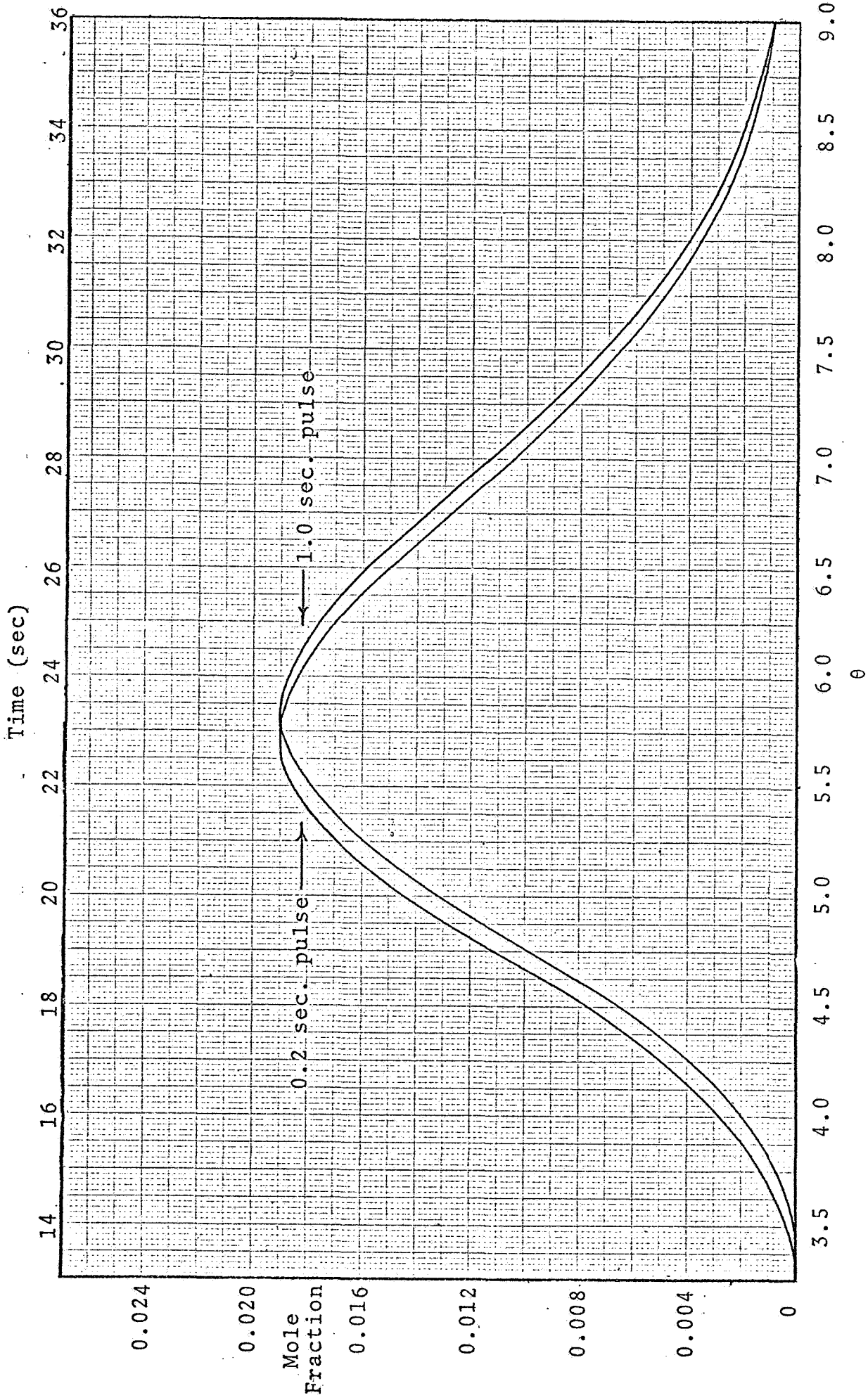


Figure 6: Equilibrium adsorption model with high diffusion,  $mR_0 = 0.2$ ,  $Pe = 60$

statement that theoretical peaks which initially are broad will not lose resolution as sample injection time increases.

A set of correlations similar to those of Figure 4 are presented in Figures 7, 8, and 9 showing how resolution is affected at different values of Pe for three values of  $mR_0$  (0.5, 0.2, 0.038). Again the effect of initial resolution is shown. At a Peclet number of 60, there is almost no initial resolution and the peak shape is unaffected by sample injection time. As Pe increases, the chromatogram becomes less broad and sample injection time becomes more important.

The effect of varying  $mR_0$  at constant Pe can also be seen in Figures 7, 8, and 9. This effect is also shown separately in Figure 10 using a slightly different correlation. This correlation can conveniently be used with the example given previously in this section. If you know from previous studies that a ratio of pulse peak height to impulse peak height of 0.9 can be tolerated, then the maximum allowable sample injection time at the specific  $mR_0$  in question can be obtained from Figure 10. One point should be noted. As  $mR_0$  increases,  $\theta_\gamma/\theta_m$  decreases. However as  $mR_0$  increases,  $\theta_m$  also decreases causing  $\theta_\gamma$  to decrease even more rapidly than would appear from the plot.

A complete solution of the second order model will tend to shift the correlations of Figure 10 to the right, thus reducing the effect of sample injection time. However,

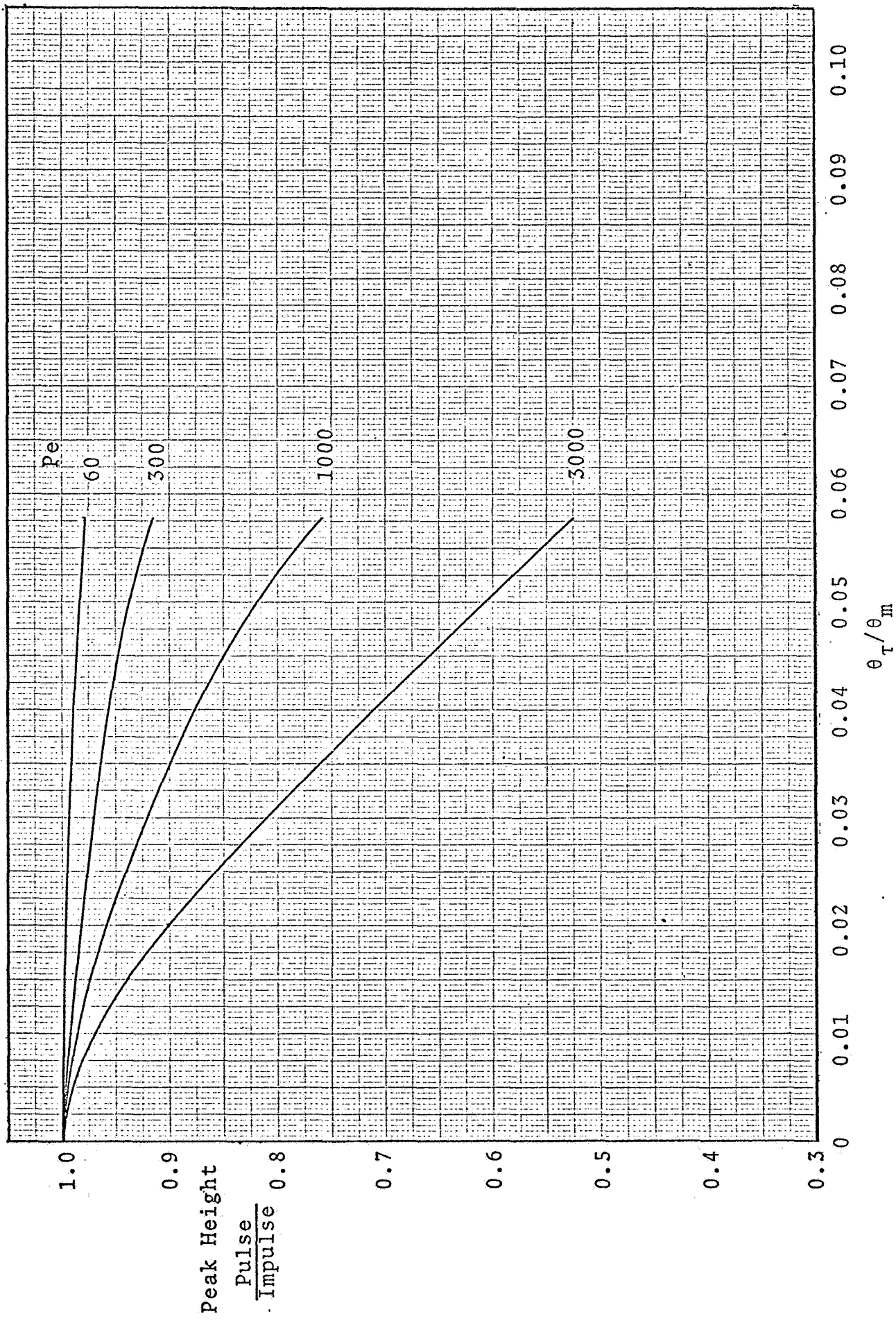


Figure 7: Effect of  $Pe$  on resolution - equilibrium adsorption model.

$mR_0 = 0.5$

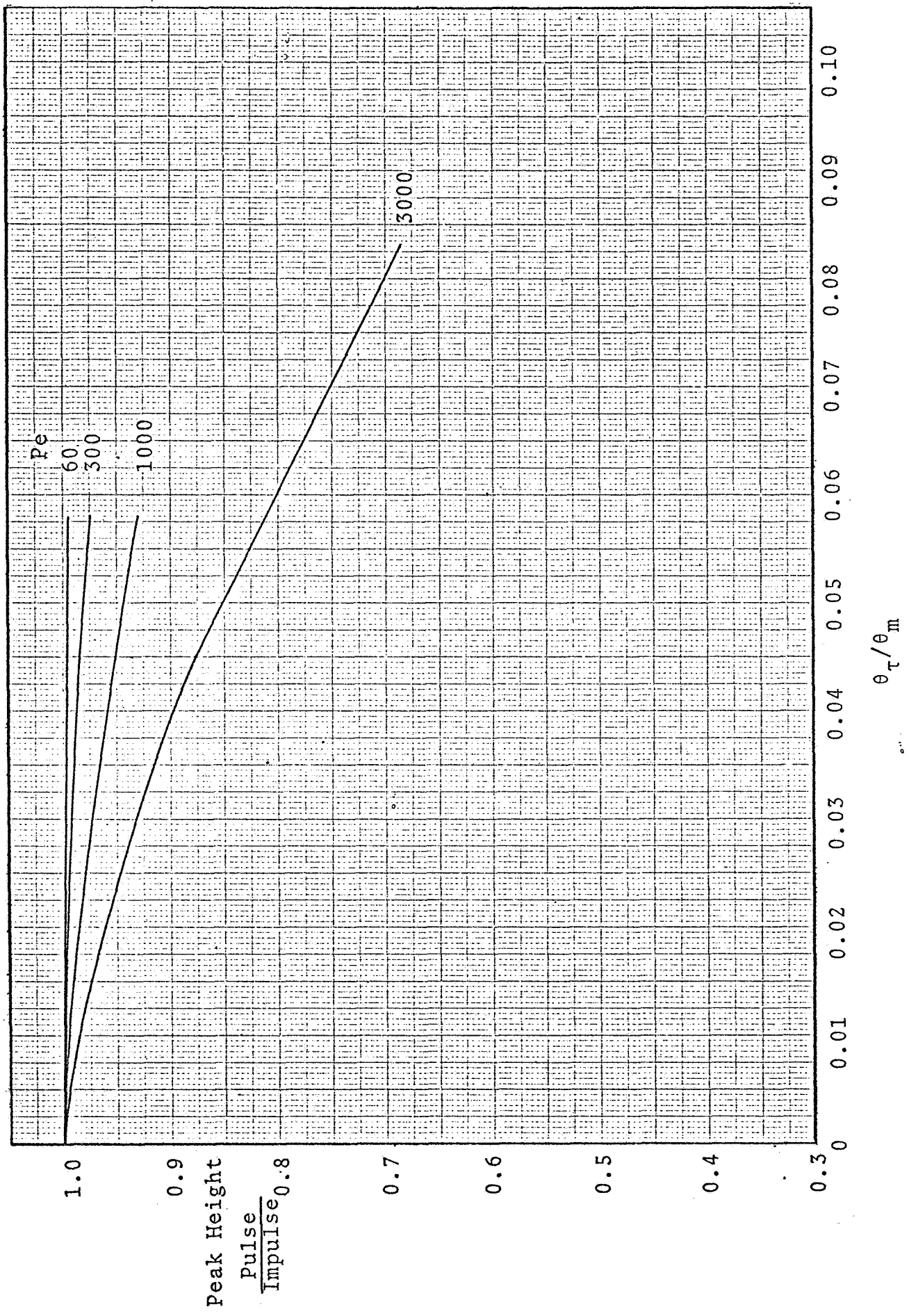


Figure 8: Effect of Pe on resolution - equilibrium adsorption model.  
 $mR_0 = 0.2$



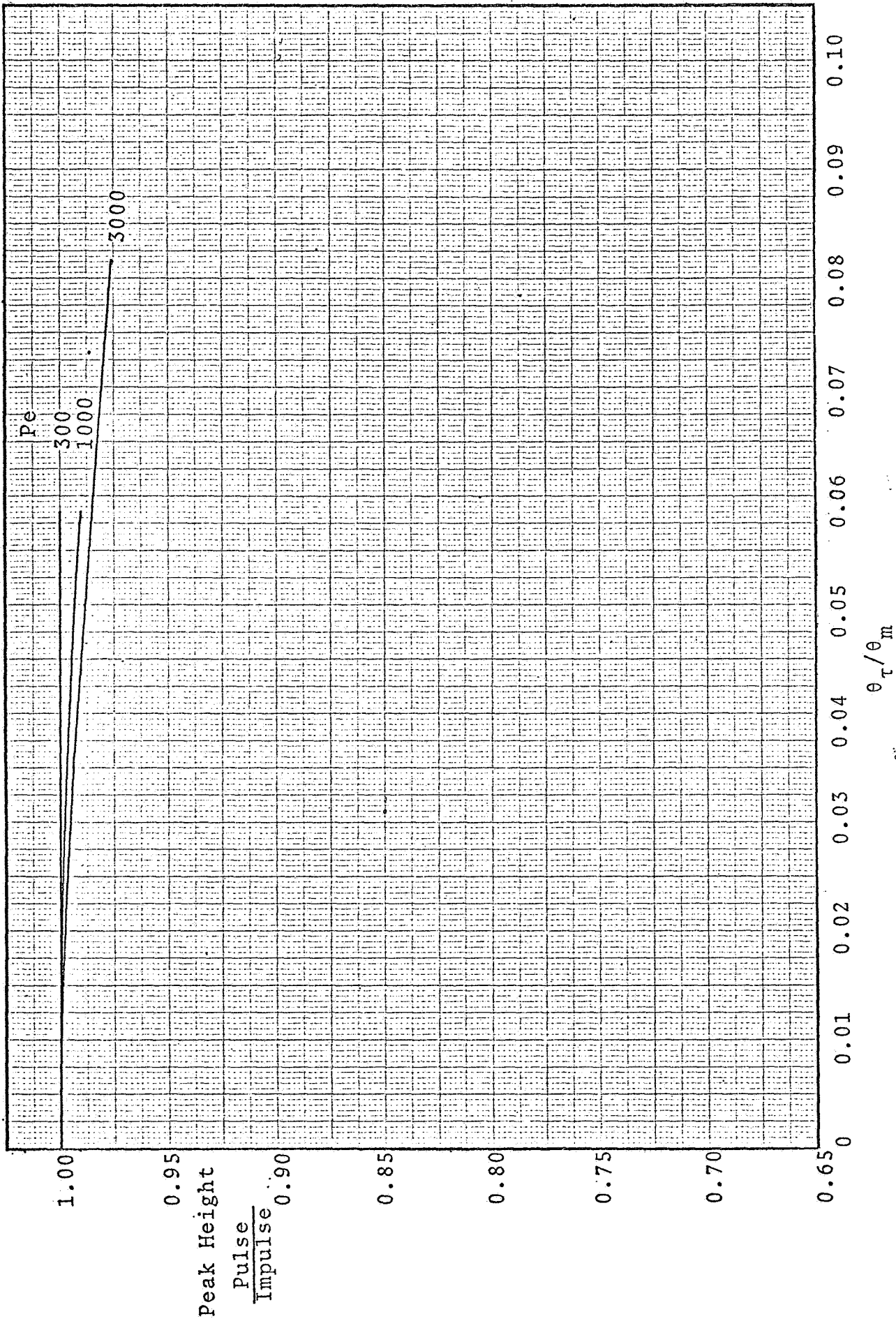


Figure 9: Effect of  $Pe$  on resolution - equilibrium adsorption model.

$mR_0 = 0.038$



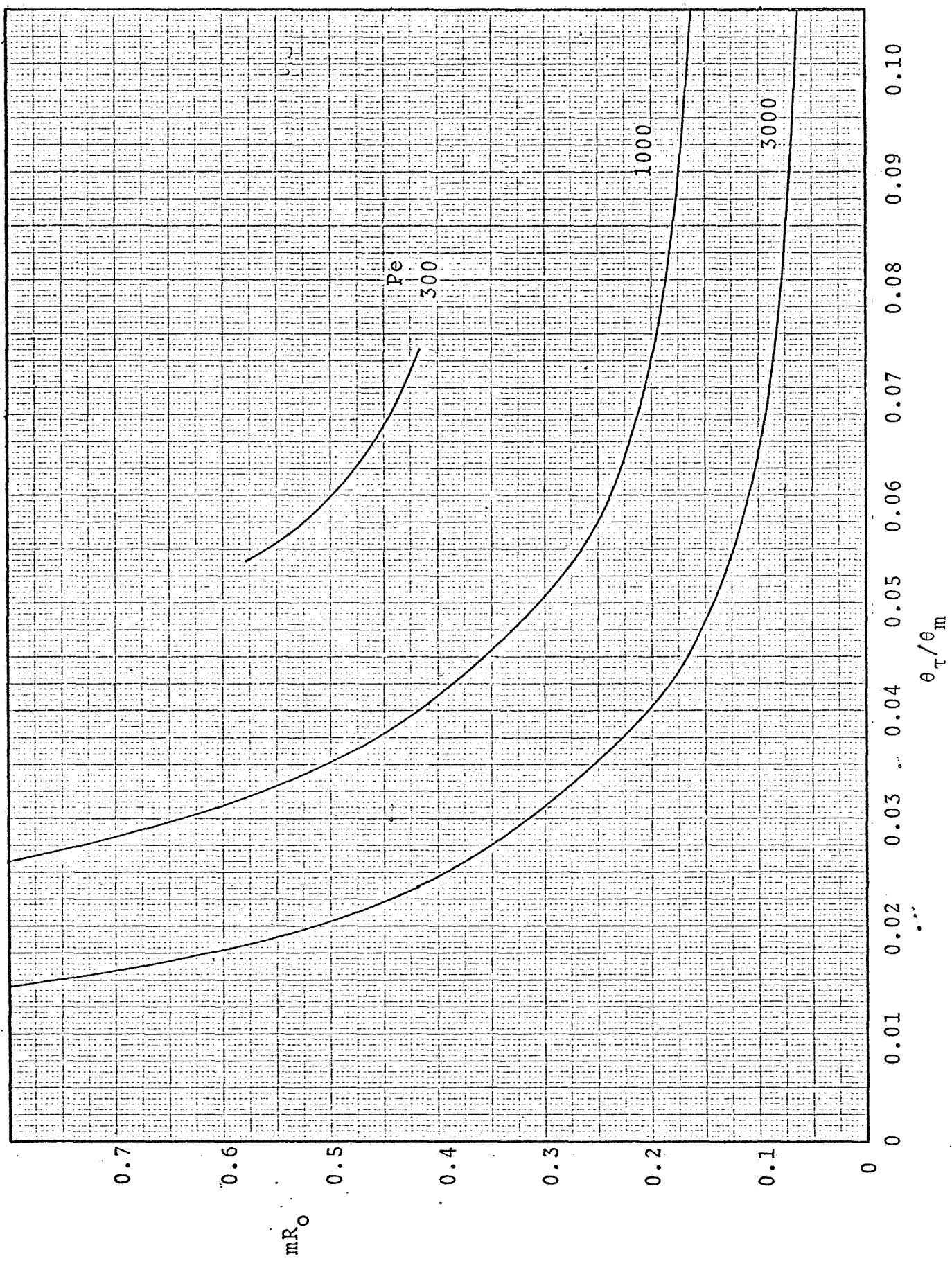


Figure 10: Effect of  $mR_0$  on  $\theta_\tau$  - equilibrium adsorption model. Peak Height  $\frac{\text{Pulse}}{\text{Impulse}} = .9$

it has been shown by use of the above techniques that sample injection time is a definite factor which must be taken into consideration if a complete description of output resolution is desired.

## PART VI

## CONCLUSIONS AND RECOMMENDATIONS

The major conclusion which must be drawn from the preceding analysis is that sample injection does have a sizeable, but varying, effect on the output chromatogram and must be included in any detailed system study in order to obtain accurate results.

Basically, increasing injection time has two effects on the chromatogram. First, because the injection function is more diffuse, the output function will be broader, and shorter since the area under each curve must be the same, the result being a loss in resolution. This loss in resolution, as compared to a peak obtained by a theoretical impulse injection, depends upon the column parameters  $P_e$ ,  $N_{tog}$ , and  $mR_0$ . Specifically, the effect of sample injection time is more noticeable as the values of the above parameters increase. No set formula has been obtained, as of now, as to how sample injection time affects a combination of the above parameters. However, as a general rule, the sharper the theoretical impulse peak (taller and narrower), the quicker that resolution is lost as a function of sample injection time. The second noticeable effect of injection time is the movement of theoretical peak times,  $\theta_m$ , to later values as the injection time increases. The cause of this phenomenon is due to the finite amount of time needed to complete the total injection of

the sample. Since the total sample is not inside the column until a time  $\theta_0$ , greater than zero, the maximum point of the output must be delayed from the theoretical peak time obtained when the total sample is injected in zero time (impulse).

Information concerning the effect of diffusion on the mathematical model was obtained when the equilibrium adsorption model of the second order system was investigated. Even though diffusional effects in the system under study are known to be small ( $Pe = 3000$ ), inclusion of these effects greatly influences the shape of the resulting chromatograms over a model which neglected them. A complete solution of the second order model should further improve the predicting of output chromatograms, hopefully to the position where the required accuracy needed for system studies can be obtained.

The technique of convoluting a pulse injection function with a mathematical model obtained using an impulse injection has proved feasible on systems other than the original first order model. Further studies using other mathematical representations of the injected function can be accomplished; however, I do not believe they will produce any more useful information than has already been obtained. It is more important to study the effect of injection upon the advanced model now being developed, so that correlations can be developed for complete system studies.

## PART VII

## NOMENCLATURE

- $A(t)$  = mathematical representation of sample injection into chromatographic column  
 $D$  = diffusion coefficient, sq ft/sec  
 $F$  = computational aid  
 $g$  = mole fraction of component in gas for pulse input  
 $I_n$  = modified Bessel function of the first kind of order  $n$   
 $J$  = computational aid  
 $L$  = length of packed bed, ft  
 $m$  = adsorption equilibrium constant,  $y^* = mX_L$   
 $N$  = sample size, lb-moles  
 $N_{\text{tog}}$  = number of transfer units available for adsorption, dimensionless  
 $Pe$  = Peclet number,  $(vL/D)$ , dimensionless  
 $R_o$  = ratio of moles of gas in bed to moles of liquid in bed  
 $s$  = Laplace transform variable, dimensionless  
 $t$  = time, sec  
 $V$  = true gas velocity, ft/sec  
 $W$  = molar flow rate of gas, lb-moles/sec  
 $x$  = position or distance in packed bed, ft  
 $X_L$  = mole fraction of component in liquid  
 $y$  = mole fraction of component in gas  
 $y^*$  = mole fraction of component in gas which is in equilibrium with liquid phase  
 $z$  = dimensionless length,  $x/L$   
 $\delta$  = variable of integration

- $\delta$  = Dirac delta function (unit impulse)
- $\theta$  = dimensionless time,  $t/(L/v)$
- $\theta_m$  = dimensionless time corresponding to maximum point on output peak
- $\theta_\tau$  = dimensionless sample injection time,  $\tau/(L/v)$
- $\lambda$  = variable of integration
- $\tau$  = sample injection time, sec

## PART VIII

## CITED LITERATURE

1. Churchill, Ruel V., "Operational Mathematics," 2nd ed., p. 35-40, McGraw-Hill Inc., New York (1958).
2. Reichman, David, "Chromatographic Systems Analysis: Evaluation of Transport Parameters," Master of Engineering Project, Rensselaer Polytechnic Institute, Troy, New York (Aug. 1969).
3. Scholly, Phillip R. and Nathaniel Brenner, "Comparative Retention Values of Representative Sample Types on Standard Gas Chromatography Columns," Instrument Society of America Proceedings, 2nd Biannual International Gas Chromatography Symposium, Volume 2, 111-140 (1959).
4. Sliva, Thomas F., "Chromatographic Systems Analysis: First-Order Model Evaluation," Master of Engineering Project, Rensselaer Polytechnic Institute, Troy, New York (Sept. 1968).
5. "System/360 Scientific Subroutine Package (360-A-CM-03X) Programmer's Manual," P. 62-63, 71-72, International Business Machines Corporation, New York (1966).
6. Voytus, Walter A., "Chromatographic Systems Analysis: Moment Analysis of the Equilibrium Adsorption Model," Master of Engineering Project, Rensselaer Polytechnic Institute, Troy, New York (June 1969).

## PART IX

## APPENDIX: COMPUTER PROGRAMS

In order to be able to convolute a rectangular pulse forcing function with the first order mathematical model, Eq. (IV-5) must be integrated. Since analytical techniques proved too bulky to manipulate, the decision was made to numerically integrate Eq. (IV-5) by means of a computer program. The technique used is that of Simpson's rule with the Bessel function expanded in an asymptotic series. The output from this program, for a specific  $N_{\text{tog}}$  and  $mR_0$ , is the cumulative area under the output chromatogram as  $\theta$  varies from zero to its final value. The technique developed in Part IV as Eq. (IV-6) can then be applied to this output, thus generating the required chromatograms for various sample injection times.

PROGRAM A and the associated BESI subroutine are specifically designed to solve Eq. (IV-5). The main program is a modification of an IBM supplied integration subroutine (5) which uses interval halving over the range of the interval (A,B) until a required accuracy is obtained. Once having computed the value of the integral (SII) for the  $i^{\text{th}}$  time the interval is halved, the interval is halved for the  $(i+1)^{\text{th}}$  time and the integral is recalculated (S). If  $|S - \text{SII}| < \text{DEL} \cdot |S|$ , where DEL is the required accuracy, then S is the final value of the integral. If the above inequality is not met, the interval is halved again until the inequality is



solved or a maximum (IMAX) number of interval halvings has taken place. The modification to the Simpson's rule program is that the total area under the chromatogram (SS) is calculated in increments of  $\Delta\theta = 0.01$  in the following manner:

$$SS = \int_0^{\theta_i} + \int_{\theta_i}^{\theta_{i+.01}} + \int_{\theta_{i+.01}}^{\theta_{i+.02}} + \dots + \int_{\theta_{i+1zz(.01)}}^{\theta_f} \quad (IX-1)$$

where  $\theta_i$  is the initial value of theta (THETA I), and  $\theta_f$  is the final value of theta (THETA F), both of which are read in as data. Each integral in the formula for SS is calculated separately according to the above procedure. After each integral is calculated, the following is written as output: upper limit of the integral (THETA), total value of SS, value of the integral in question (S), and the total number of increments into which the integral was divided (N).

The BESI subroutine used with PROGRAM A is also a modification of an IBM supplied subroutine (5) which will compute  $I_1(\lambda)$  of Eq. (IV-5). The modifications are as follows. The IBM program computes  $I_n(\lambda)$  in a series approximation if  $\lambda \leq 12 \leq n$ , and in an asymptotic approximation if  $\lambda > 12 > n$ . The series approximation has been dropped from the BESI subroutine of PROGRAM A due to underflows which developed; however, this has no effect on the accuracy of the computations. The only place in which the series approximation is used is near the lower limit in the first integral of Eq. (IX-1). Since the value which is computed for  $I_n(\lambda)$  is extremely

small in this region (less than  $10^{-75}$ ), no accuracy is lost if zero is returned to the main program as the value of  $I_n(\lambda)$ . The resulting approximation for  $I_n(\lambda)$  is:

$$I_n(\lambda) = \frac{e^\lambda}{\sqrt{2\pi\lambda}} \sum_{m=0}^{30} (8\lambda)^{-m} \frac{1}{m!} \prod_{K=1}^m \left[ (2K-1)^2 - 4n^2 \right] \quad (\text{IX-2})$$

The second modification is the fact that  $I_1(\lambda)$  is not the complete integrand. We desire to integrate the function:

$$\exp \left[ - \left( \frac{\lambda}{2\sqrt{N_{\text{togz}}}} \right)^2 - N_{\text{togz}} \right] I_1(\lambda) \quad (\text{IX-3})$$

Therefore, in the subroutine the exponential term of Eq. (IX-2) is combined with the exponential of Eq. (IX-3), as XYZ, and the whole value of Eq. (IX-3) is returned, as BI, to the main program. If XYZ is less than -150, EXP(XYZ) is approximately  $10^{-70}$ , therefore the value of BI is returned as zero. If XYZ is greater than 174, EXP(XYZ) is larger than  $10^{75}$  and an error indicator is set causing the main program to print out this fact.

PROGRAM B calculates directly the output chromatogram for an impulse injection (of sample size equal to 1.0) at a specific  $N_{\text{tog}}$  and  $mR_0$ . The program operates exactly in the same manner as the BESI subroutine and is subject to the same modifications. The output of this program is a list of  $\theta$ 's, from the initial to the final value, with the corresponding mole fraction value (Y) of the impulse chromatogram, where Y is defined by Eq. (III-5) with the sample size term set equal to 1.0.

PROGRAM C is the counterpart of PROGRAM A for the equilibrium adsorption case Eq. (III-6). The main program, with a few minor changes is exactly the same as the main program of PROGRAM A. The subroutine (RCK) is a straightforward calculation of the function to be integrated with a similar check on the bounds of the exponential term (A) as is found in the BESI subroutine. Output of PROGRAM C is exactly the same as that of PROGRAM A.

None of the above programs are in their most efficient form. They are written specifically to solve a certain set of equations and are included only as a guide to the results of Part V, and a reference to be used when the complete mathematical model is developed.

DATA CARD FORMATS

All three programs are designed to operate on any number of data sets. Each data card (after the first) contains all of the information necessary to cause a complete run of the program. Each program will cycle over the total number of data cards designated by the first card read.

Input for PROGRAM A and PROGRAM B

```

Card 1
      col 1-5 total number of data cards following (I5)
Card 2,3,...
      col 1-10  $N_{\text{tog}}$  (F10.5)
           11-20  $mR_0$  (F10.5)
           21-30 starting value of  $\theta$  (F10.5)
           31-40 final value of  $\theta$  (F10.5)
           41-50 z-dimensionless distance (F10.5)

```

Input for PROGRAM C

```

Card 1
      col 1-5 total number of data cards following (I5)
Card 2,3,...
      col 1-10  $Pe$  (F10.5)
           11-20  $mR_0$  (F10.5)
           21-30 starting value of  $\theta$  (F10.5)
           31-40 final value of  $\theta$  (F10.5)

```

VARIABLE LISTING FOR ALL COMPUTER PROGRAMS

A = lower limit of the integral when used in main programs  
 = value of exponential term when used in subroutine RCK  
 AA = integrand value found at the lower limit of the integral  
 AMRO =  $mR_0$  - measure of component volatility  
 ANHLEF = floating point value of NHALF  
 ANTOG =  $N_{tog}$  - total number of column transfer units  
 B = upper limit of the integral  
 BA = difference between integral limits  
 BESI = subroutine name used in the first order program  
 BI = value of integrand returned to the main program  
 DEL = tolerance factor used in Simpson's rule integral  
 FINC = size of each interval increment  
 FK = factor used in the asymptotic Bessel function series  
 FN = set value determined by the order of the Bessel function  
 FRSTX = point at which integrand value is to be determined  
 G = dimensionless time of theoretical peak occurrence  
 I =  $D\emptyset$  loop counter  
 IER = error indicator in BESI: 0 = no error  
           1 = order of Bessel function  
                   is less than zero  
           2 = Bessel function argument  
                   less than zero  
           3 = XYZ has a value less than  
                   -150  
           4 = XYZ has a value greater  
                   than 174  
 IMAX = maximum number of interval halvings allowable for  
           each integral  
 INZZ =  $D\emptyset$  loop counter running over the total number of  
           data cards read  
 ITHETA =  $D\emptyset$  loop counter

IZZ = total number of  $\theta$  increments inner  $D\theta$  loop operates over  
 K =  $D\theta$  loop counter  
 KLAST = last increment point at which integrand value is to be determined  
 N = total number of increments the integral is divided into  
 NHALF = number of times the integral interval is halved  
 NZZ = total number of data cards to be read  
 PE = Peclet number  
 PI =  $\pi$   
 RCK = subroutine name used in the equilibrium adsorption program.  
 S = value of the integral found in the present approximation  
 SII = value of the integral found in the previous approximation  
 SS = summational variable - contains total value of all integrals  
 SUMK = value of integral at various points  
 TERM = one term of the asymptotic Bessel function series.  
 THETA =  $\theta$ , dimensionless time  
 THETAF = final value of  $\theta$  at which the program stops  
 THETA I = initial value of  $\theta$  at which the program starts  
 TOL = tolerance used in various determinations  
 X = midpoint of integral limits when used in the main programs  
 = value upon which subroutines act when used in subroutines  
 =  $2Nt_{\text{og}} \sqrt{mR_0 z(\theta - z)}$  when used in PROGRAM B  
 XK = counter running over all increments of the integral  
 XX = multiplying factor in asymptotic Bessel function series  
 XYZ = argument of the exponential term  
 Y = final value in mole fraction (for a sample size of 1) of the impulse peak at the  $\theta$  in question  
 Z = dimensionless distance down the column

PROGRAM A

```

READ(1,1)NZZ
1 FORMAT(I5)
DO 29 INZZ=1,NZZ
  READ(1,2)ANTOG,AMRO,THETA,THETA,Z
2 FORMAT(5F10.5)
  WRITE(3,3)ANTOG,AMRO,Z
3 FORMAT(/////,10X,'NTOG = ',F10.1,5X,'MRO = ',F10.5,5X,
1 'Z = ',F10.5,/)
  WRITE(3,4)
4 FORMAT(10X,'THETA',10X,'SUMMATION',22X,'INTEGRAL',10X,'N',/)
  IZZ=((THETA-THETA)*100.)+0.01
  SS=0.0
  DO 28 ITHETA=1,IZZ
    THETA=(THETA-0.01)+(ITHETA*0.01)
    B=2.*ANTOG*SQRT(AMRO*Z*(THETA-Z))
    IF(ITHETA-1)6,5,6
5 A=0.0
  GO TO 7
6 A=2.*ANTOG*SQRT(AMRO*Z*(THETA-Z-0.01))
7 DEL=0.001
  IMAX=10
  SII=0.0
  S=0.0
  N=0
  BA=B-A
  IF(BA)8,8,10
8 WRITE(3,9)
9 FORMAT(20X,'A=B, OR A IS GREATER THAN B      PROGRAM TERMINATED')
  CALL EXIT
10 X=BA/2.+A
  NHALF=1
  CALL BESI(X,1,BI,IER,ANTOG,Z)
  IF(IER)21,11,21
11 SUMK=BI*BA*2./3.
  CALL BESI(A,1,BI,IER,ANTOG,Z)
  IF(IER)21,12,21
12 AA=BI
  CALL BESI(B,1,BI,IER,ANTOG,Z)
  IF(IER)21,13,21
13 S=SUMK+(AA+BI)*BA/6.
  DO 17 I=2,IMAX
    SII=S
    S=(S-SUMK/2.)/2.
    NHALF=NHALF*2
    ANHLF=NHALF
    FRSTX=A+(BA/ANHLF)/2.
    CALL BESI(FRSTX,1,BI,IER,ANTOG,Z)
    IF(IER)21,14,21

```

```

14 SUMK=BI
   XK=FRSTX
   KLAST=NHALF-1
   FINC=BA/ANHLEF
   DO 15 K=1,KLAST
   XK=XK+FINC
   CALL BESI(XK,1,BI,IER,ANTOG,Z)
   IF(IER)21,15,21
15 SUMK=SUMK+BI
   SUMK=SUMK*2.*BA/(3.*ANHLEF)
   S=S+SUMK
16 IF(ABS(S-SII)-ABS(DEL*S))19,19,17
17 CONTINUE
   WRITE(3,18)
18 FORMAT(20X,'REQUIRED ACCURACY NOT MET IN IMAX STEPS')
19 N=2*NHALF
   S=SS+S
   SS=S
   WRITE(3,20)THETA,SS,S,N
20 FORMAT(10X,F5.2,E20.5,20X,E20.5,I10)
   GO TO 28
21 GO TO (22,22,24,26),IER
22 WRITE(3,23)
23 FORMAT(20X,'ERROR IN BESI SUBROUTINE. PROGRAM TERMINATED')
   CALL EXIT
24 SS=0.0
   WRITE(3,25)THETA,SS
25 FORMAT(10X,F5.2,E20.5)
   GO TO 28
26 WRITE(3,27)THETA
27 FORMAT(10X,F5.2,9X,'GREATER THAN 10**75')
28 CONTINUE
29 CONTINUE
   CALL EXIT
   END

```

```

SUBROUTINE BESI(X,N,BI,IER,ANTOG,Z)
  IER=0
  BI=1.0
  IF(N)15,2,1
1 IF(X)16,4,4
2 IF(X)16,3,4
3 RETURN
4 TOL=1.0E-3
  IF(X-12.)6,6,5
5 IF(X-FLOAT(N))6,6,7
6 BI=0.0
  GO TO 17

```



```
7 FN=4*N*N
  XX=1./(8.*X)
  TERM=1.0
  BI=1.0
  DO 9 K=1,30
  IF(ABS(TERM)-ABS(TOL*BI))10,10,8
8 FK=(2*K-1)**2
  TERM=TERM*XX*(FK-FN)/FLOAT(K)
9 BI=BI+TERM
10 PI=3.141592653
  XYZ=X-(X/(2.*SQRT(ANTOG*Z)))**2-ANTOG*Z
  IF(150.+XYZ)11,12,12
11 BI=0.0
  GO TO 17
12 IF(XYZ-174.)14,14,13
13 IER=4
  GO TO 17
14 BI=BI*EXP(XYZ)/SQRT(2.*PI*X)
  GO TO 17
15 IER=1
  GO TO 17
16 IER=2
17 RETURN
  END
```

PROGRAM B

```

READ(1,1)NZZ
1 FORMAT(I5)
DO 16 INZZ=1,NZZ
  READ(1,2)ANTOG,AMRO,THETA,THETA,Z
2 FORMAT(5F10.5)
  WRITE(3,3)ANTOG,AMRO,Z
3 FORMAT(/////10X,'NTOG = ',F10.1,5X,'MRO = ',F10.5,5X,
1 'Z = ',F10.5,/)
  TOL=1.0E-3
  WRITE(3,4)
4 FORMAT(10X,'THETA',14X,'Y',/)
  IZZ=((THETA-THETA)*100.)/0.01
  DO 15 ITHETA=1,IZZ
  THETA=(THETA-0.01)+(ITHETA*0.01)
  X=2*ANTOG*SQRT(AMRO*Z*(THETA-Z))
  BI=1.0
  FN=4.0
  XX=1./(8.*X)
  TERM=1.0
  DO 6 K=1,30
  IF(ABS(TERM)-ABS(TOL*BI))7,7,5
5 FK=(2*K-1)**2
  TERM=TERM*XX*(FK-FN)/FLOAT(K)
6 BI=BI+TERM
7 PI=3.141592653
  XYZ=X-(ANTOG*Z)-((THETA-Z)*ANTOG*AMRO)
  IF(150.+XYZ)8,9,9
8 BI=0.0
  GO TO 13
9 IF(XYZ-174.)12,12,10
10 WRITE(3,11)
11 FORMAT(10X,'XYZ TO LARGE')
  GO TO 15
12 BI=BI*EXP(XYZ)/SQRT(2.*PI*X)
13 Y=2.*ANTOG*ANTOG*Z*AMRO*BI/X
  WRITE(3,14)THETA,Y
14 FORMAT(10X,F5.2,E20.5)
15 CONTINUE
16 CONTINUE
  CALL EXIT
  END

```

PROGRAM C

```

READ(1,1)NZZ
1 FORMAT(I5)
DO 20 INZZ=1,NZZ
  READ(1,2)PE,AMRO,THETA1,THETA F
2 FORMAT(4F10.5)
  WRITE(3,3)PE,AMRO
3 FORMAT(//////,10X,'PECLET NUMBER = ',F10.1,5X,'MRO = ',F10.5,/)
  WRITE(3,4)
4 FORMAT(10X,'THETA',10X,'SUMMATION',22X,'INTEGRAL',10X,'N',/)
  IZZ=((THETA F-THETA1)*100.)÷0.01
  G=1.0+(1.0/AMRO)
  SS=0.0
  DO 19 ITHETA=1,IZZ
    THETA=(THETA1-0.01)+(ITHETA*0.01)
    B=THETA
    IF(ITHETA-1)6,5,6
5 A=0.0
  GO TO 7
6 A=THETA-0.01
7 DEL=0.001
  IMAX=10
  SII=0.0
  S=0.0
  N=0
  BA=B-A
  IF(BA)8,8,10
8 WRITE(3,9)
9 FORMAT(20X,'A=B, OR A IS GREATER THAN B   PROGRAM TERMINATED')
  CALL EXIT
10 X=BA/2.+A
  NHALF=1
  CALL RCK(X,BI,PE,G)
  SUMK=BI*BA*2./3.
  IF(A)12,11,12
11 BI=0.0
  GO TO 13
12 CALL RCK(A,BI,PE,G)
13 AA=BI
  CALL RCK(B,BI,PE,G)
  S=SUMK+(AA+BI)*BA/6.
  DO 15 I=2,IMAX
    SII=S
    S=(S-SUMK /2.)/2.
    NHALF=NHALF*2
    ANHLF=NHALF
    FRSTX=A+(BA/ANHLF)/2.
    CALL RCK(FRSTX,BI,PE,G)
    SUMK=BI
    XK=FRSTX

```

```

KLAST=NHALF-1
FINC=BA/ANHLLF
DO 14 K=1,KLAST
XK=XK+FINC
CALL RCK(XK,BI,PE,G)
14 SUMK=SUMK+BI
SUMK=SUMK*2.*BA/(3.*ANHLLF)
S=S+SUMK
IF(ABS(S-SII)-ABS(DEL*S))17,17,15
15 CONTINUE
WRITE(3,16)
16 FORMAT(20X,'REQUIRED ACCURACY NOT MET IN IMAX STEPS')
17 N=2*NHALF
S=SS+S
SS=S
WRITE(3,18)THETA,SS,S,N
18 FORMAT(10X,F5.2,E20.5,20X,E20.5,I10)
19 CONTINUE
20 CONTINUE
CALL EXIT
END

```

```

SUBROUTINE RCK(X,BI,PE,G)
A=(PE/2.)-((PE*X)/(4.*G))-((PE*G)/(4.*X))
IF(150.*A)1,2,2
1 BI=0.0
GO TO 6
2 IF(A-174.)5,5,3
3 WRITE(3,4)
4 FORMAT(///,30X,'*****',/,10X,'EXPONENTIAL IN SUB
1ROUTINE IS GREATER THAN 10**75',/,30X,'*****')
CALL EXIT
5 BI=SQRT((G*PE)/(3.14159*(X**3)))*EXP(A)*0.5
6 RETURN
END

```